

## EFFECT OF SINTERING TEMPERATURE ON V<sub>2</sub>O<sub>5</sub> DOPED ZnO-Bi<sub>2</sub>O<sub>3</sub>-Sb<sub>2</sub>O<sub>3</sub>-MnO<sub>2</sub> BASED VARISTOR CERAMICS: MICROSTRUCTURE AND ELECTRICAL PROPERTIES

D. UMARU<sup>a</sup>, A. ZAKARIA<sup>b\*</sup>, C. A. C. ABDULLAH<sup>c</sup>, I. I. LAKIN<sup>d</sup>,  
Y. ABDOLLAHI<sup>e</sup>

<sup>a</sup>Department of Physics, Faculty of Science, Universiti Putra Malaysia, 43400 UPM Serdang, Selangor, Malaysia

<sup>b</sup>Department of Physics, Faculty of Science, Universiti Putra Malaysia, 43400 UPM Serdang, Selangor, Malaysia

<sup>c</sup>Synthesis and characterization laboratory, Institute of Advanced Technology, Universiti Putra Malaysia, 43400 UPM Serdang, Selangor, Malaysia

<sup>d</sup>Department of Physics, Faculty of Science, Universiti Putra Malaysia, 43400 UPM Serdang, Selangor, Malaysia

<sup>e</sup>Department of Electrical Engineering, Faculty of Engineering, University of Malaya, 50603 Kuala Lumpur, Malaysia

In this study the effect of the sintering temperature (1200–1300 °C) on V<sub>2</sub>O<sub>5</sub> doped ZnO–Bi<sub>2</sub>O<sub>3</sub>-Sb<sub>2</sub>O<sub>3</sub>-MnO<sub>2</sub> (ZBSM) based varistor ceramics from 0 to 0.4 mol% was investigated for electrical and microstructural properties. The materials was processed using a conventional solid-state method and the finished samples were characterized using XRD, SEM and EDX techniques. The measured leakage current density was  $1 \times 10^{-4}$  mA/cm<sup>2</sup> when the barrier height was 1.38 eV, which gave the highest nonlinear coefficient around 12.18 at 0.20 mol%. The analyses related to those quoted in the literatures confirmed the presence of Zn<sub>7</sub>Sb<sub>2</sub>O<sub>12</sub>, MnVO<sub>4</sub>, BiVO<sub>4</sub> and Zn<sub>3</sub>(VO<sub>4</sub>)<sub>2</sub> polymorphs as the secondary phase with ZnO as the primary phase. The Zn<sub>3</sub>(VO<sub>4</sub>)<sub>2</sub> polymorphs resided at the triple point junctions or were embedded in ZnO grains. Henceforth, the results showed that V<sub>2</sub>O<sub>5</sub> doping can facilitate the sintering process of the varistor ceramics, particularly in the phase formation. This contributed to better electrical properties, especially to 0.2 mol%. The density of the sintered ceramic decreased from 5.32 to 5.06 g/cm<sup>3</sup> and the average grain size increased in the range of 11.02 to 31.39 μm with an increased of sintering temperature from 1200 to 1300 °C, respectively.

(Received April 24, 2016; Accepted July 4, 2016)

**Keywords:** Zinc oxide varistor, V<sub>2</sub>O<sub>5</sub>, sintering temperature, ZBSM

### 1. Introduction

Zinc oxide (ZnO) based varistors are electronic semiconducting ceramic materials that possess high energy absorption capability to protect electronic appliances against an unwanted voltage surge transmitted into the electronic components that can possibly cause damage [1]. They are simply achieved by sintering a ZnO powder mix with some minor metallic oxides. Moreover, ZnO varistor materials form a polycrystalline structure after sintering, consisting of semiconductor ZnO grains [2]. The type of additives used is greatly important in its fabrication, leading to the formation of secondary phases at the grain boundary that trigger the J-E characteristics [3].

Generally, the electrical properties, such as nonlinear coefficient ( $\alpha$ ), leakage current density ( $J_l$ ), breakdown field ( $E_b$ ), and barrier height ( $\phi_b$ ) are controlled by the structure of the

grains and grain boundaries, mostly originating from the segregation of heavy metal oxide, such as  $\text{Bi}_2\text{O}_3$ ,  $\text{Pr}_6\text{O}_{11}$  and  $\text{V}_2\text{O}_5$ , on ZnO grains or grain boundary [4-5]. The nonlinear current density-electric field (J-E) characteristics of a ZnO based varistor is determined from the total number of grain-boundary layers that can be generated during the sintering process, including the formation of the electronic  $\phi_b$  [6]. Consequently, the addition of minor oxides of  $\text{MnO}_2$  in small percentages can avoid  $\text{Bi}_2\text{O}_3$  and  $\text{V}_2\text{O}_5$  evaporation during the sintering process [7]; also,  $\text{Sb}_2\text{O}_3$  addition leads to the formation of a  $\text{Zn}_7\text{Sb}_2\text{O}_{12}$  spinel phase which reduces the mobility of the grain boundaries and regulates the ZnO grain growth [8-9].

Recent studies have revealed that  $\text{V}_2\text{O}_5$  along with a varistor previously added on ZnO has the advantage in terms of lowering the sintering temperature, but there is no improvement in the electrical properties. There is a need for incorporation of many additives to improve the  $\alpha$  of the varistor [10, 11, 12]. Accordingly, the combined effects of  $\text{MnO}_2$ ,  $\text{Pr}_6\text{O}_{11}$ ,  $\text{Co}_3\text{O}_4$  and  $\text{Sb}_2\text{O}_3$  on the ZnO- $\text{V}_2\text{O}_5$  contributes to the varistor  $E_b$  potential, which acts from highly resistive to extremely conductive; also, the ceramic can be sintered at a high temperature of above 1250 °C [12, 13, 14].

Although, the effect of the sintering temperature on  $\text{V}_2\text{O}_5$  doped ZnO- $\text{Bi}_2\text{O}_3$ - $\text{Sb}_2\text{O}_3$ - $\text{MnO}_2$  (ZBSM) based varistor ceramics has not been studied symmetrically, there has been a report in literature on the combined effect of ZnO- $\text{V}_2\text{O}_5$ - $\text{MnO}_2$ - $\text{Nb}_2\text{O}_5$ - $\text{Bi}_2\text{O}_3$  ceramics, recently [15]. In addition the combined effect of ZnO- $\text{V}_2\text{O}_5$ - $\text{MnO}_2$ - $\text{Nb}_2\text{O}_5$  ceramics was reported [16].  $\text{Mn}_3\text{O}_4$  doping in ZnO- $\text{V}_2\text{O}_5$  varistor ceramics was also reported to control ZnO abnormal grain growth [17]. As reported earlier, incorporation of  $\text{V}_2\text{O}_5$  additives markedly enhanced the densification rate of the ZnO materials [18]. Also, the grain-growth rate of the ZnO materials was significantly increased because  $\text{V}_2\text{O}_5$  acted as a liquid phase sintering.

Generally,  $\text{V}_2\text{O}_5$  improved the electrical properties in particular the nonlinear J-E characteristics of ZnO based varistor ceramics [19]. Another important parameter to be considered is the microstructural properties in which the varistor electrical properties can be determined, particularly the J-E characteristics of the ZnO based varistor ceramics. The responsible mechanism is the grain boundary; better grain boundaries produce optimum nonlinear J-E characteristics [20-21].

Recently, the investigation on the effect of  $\text{V}_2\text{O}_5$  doped ZnO at 0.5 mol% and low sintering temperature has received major attention in specific the degradation behavior, electrical properties and microstructure [22, 23, 24]. However, many problems related to ZnO based varistors such as abnormal grain boundaries need to be solved in order to use them for commercial purposes. The selected type of sintering process for a specific composition is needed in order to improve the  $\alpha$  of ZnO- $\text{V}_2\text{O}_5$  based ceramics [22]. As a result, it is significant to investigate how a small amount of  $\text{V}_2\text{O}_5$ , between 0.08 to 0.4 mol%, will significantly affect the performance of ZnO varistor properties in different sintering temperatures.

Numerous processing conditions have been established to improve the microstructural and electrical properties of ZnO varistor ceramics; several studies discovered that had a combined effect of ZnO- $\text{V}_2\text{O}_5$ - $\text{MnO}_2$  varistor ceramics sintered between 1200-1300 °C for 4 hrs and the holding time did not give any nonlinear electrical properties [19, 25]. The effect of the sintering temperature on the additive of  $\text{V}_2\text{O}_5$  commonly found in the well-studied ZBSM is still not reported in literatures.

In this work, a study on the effect of sintering temperature on  $\text{V}_2\text{O}_5$  doped on ZBSM based varistor ceramics has been systematically studied for different sintering temperatures, and for its dependence on electrical and microstructure properties. It is unique compared with those previous works in term of the processing conditions; sintering temperature, sintering time, and additives. Here, the sintering temperature, time and selected of  $\text{V}_2\text{O}_5$  doping used were >1200 °C, 4 h, and 0.2 mol%, respectively, compared to that of others were 900 °C, 10 min, and 0.5 mol% [18]. We expected that the electrical properties, particularly  $\alpha$ , would increase to an optimum with the increase of sintering temperature and doping.

## 2. Experimental procedure

A high purity of metal oxide powders were obtained from Sigma-Aldrich; ZnO (99.9%), V<sub>2</sub>O<sub>5</sub> (99.6%), Bi<sub>2</sub>O<sub>3</sub> (99.98%), Sb<sub>2</sub>O<sub>3</sub> (99.6%) and MnO<sub>2</sub> (86.93%), and the design ceramic system is ZnO<sub>(98.8-x)</sub>V<sub>2</sub>O<sub>5(x)</sub>Bi<sub>2</sub>O<sub>3(0.7)</sub>MnO<sub>2(0.7)</sub>Sb<sub>2</sub>O<sub>3(0.3)</sub> where x is varied from 0.08 to 0.4 mol% at chosen sintering temperature 1250 °C. Later at an optimum x mol% of V<sub>2</sub>O<sub>5</sub> in ZBSM ceramic the sintering temperature was varied between 1200 to 1300 °C to obtain further optimum in microstructure and electrical properties. The raw materials were mixed by ball-milling with zirconia balls in a polypropylene bottle for 24 h in acetone and a small addition of deionized water to avoid the sedimentation of heavy particles like Sb<sub>2</sub>O<sub>3</sub>. 0.75wt% polyvinyl alcohol as binder was added. The mixture was dried at 110 °C for 19 h in an oven and granulated using an agate mortar/pestle. The powder was sieved with a 75 micron mesh screen to produce the starting powder. The powder was pressed into discs (pellets) of 10 mm diameter and 1 mm thickness at a pressure of 50 MPa. The pellets were sintered in air in intervals of 4 h, with heating and cooling rates of 5 °C/min and finally, furnace-cooled to room temperature. The sintered samples were polished to a 0.89 mm thickness using SiC paper, P1200. For electroding, silver paste was coated on both side of its faces for areas of approximately 0.238 cm<sup>2</sup> and then heated at 550 °C for 12 min to form ohmic contacts.

### 2.1 Characterization method

The J-E characterization of the samples was recorded at room temperature by using a source measure unit (Keithley 2400). From it, the constant  $\alpha$  was obtained by using the expression [26];

$$J = aE^\alpha \quad (1)$$

or

$$\alpha = \frac{(\log J_2 - \log J_1)}{(\log E_2 - \log E_1)} \quad (2)$$

where the varistor electric fields  $E_2$ ,  $E_1$  were taken at current densities  $J_2 = 10 \text{ mA/cm}^2$ ,  $J_1 = 1 \text{ mA/cm}^2$ , and the  $J_L$  was evaluated at  $0.85V_{1mA}$

Scanning electron microscope (SEM, JEOL JSM-6400) in conjunction with energy dispersive X-ray (EDX) was used to determine the morphological structure and elements within the composition. The XRD pattern of the prepared samples was recorded using (PANalytical X'Pert Pro PW3040/60, Philips). The samples were radiated with Ni-filtered CuK $\alpha$  radiation ( $\lambda = 1.5428 \text{ \AA}$ ) within a  $2\theta$  scan range of 20 - 80° to identify the crystalline phases; the data were analyzed using X'Pert High Score software. The density of the sintered pellets was measured with a digital electronic densitometer, and the average grain size was calculated by using the linear intercept method [27],[28].

$$d = \frac{1.56L}{MN} \quad (3)$$

where L is the random line length on the micrograph, M is the micrograph magnification and N is the number of grain boundaries intercepted by lines.

## 3. Results and discussion

### 3.1 Phase identification

Fig. 1(a) shows the XRD pattern of phases obtained by the doping x of 0.08, 0.2, 0.4 mol% V<sub>2</sub>O<sub>5</sub> composition in ZBSM ceramics sintered at a chosen sintering temperature which is 1250 °C. Fig. 1(b) is the pattern of sample produced from five sintering temperatures, 1200 to 1300 °C, for the selected x=0.2 mol% V<sub>2</sub>O<sub>5</sub> based on the

optimum  $\alpha$  from E-J characteristic. A strong peak related to the  $\text{Zn}_3(\text{VO}_4)_2$  minor phase was detected. Usually,  $\text{Zn}_3(\text{VO}_4)_2$  is found to be fixed in ZnO grains or at triple point junction grains [7, 24]. The existence of  $\text{Zn}_3(\text{V}_4)_2$  could not be confirmed by XRD analysis at 1300 °C due to the volatility of the V-species; also, the main peak of  $\text{Zn}_3(\text{VO}_4)_2$  had already overlapped with those of the  $\text{Zn}_7\text{Sb}_2\text{O}_{12}$  spinel.

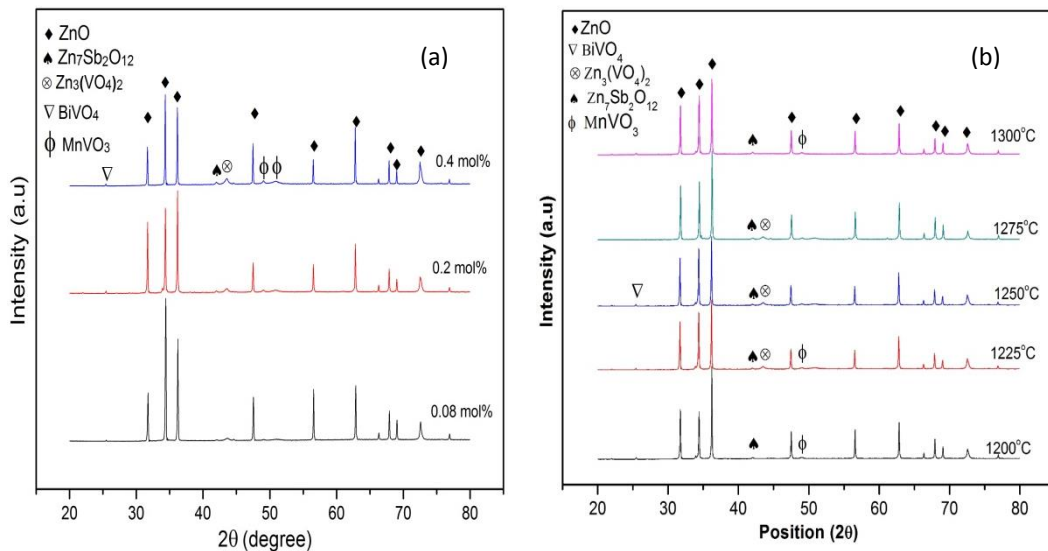


Fig. 1: Shows XRD peaks of the sample, (a) sintered at 1250 °C of three different mol%  $\text{V}_2\text{O}_5$  (0.08 - 0.4) and (b) doped at 0.2 mol%  $\text{V}_2\text{O}_5$  sample sintered at five different temperatures.

The trace for elevated temperatures revealed the presence of ZnO as the only primary phase; and, a few secondary phases, such as,  $\text{BiVO}_4$ ,  $\text{MnVO}_3$  and  $\text{Zn}_3(\text{VO}_4)_2$  polymorphs, related to the V and  $\text{Zn}_7\text{Sb}_2\text{O}_{12}$  species as the only secondary phases were detected. The presence of  $\text{BiVO}_4$  shows that Bi and V-rich, a liquid phase sintering, has aided this result to be consistent with [15]. The formation of the  $\text{Zn}_7\text{Sb}_2\text{O}_{12}$  spinel phase at 1200 °C, the initial temperature, until 1300 °C was found to control the abnormal ZnO grain growth and enhance the sintering process for the solubility of ions, such as the Zn and Bi-reach liquid phase, which were reported from literatures [26, 9]. The indexed spinel phase of  $\text{Zn}_7\text{Sb}_2\text{O}_{12}$  obtained was a cubic structure with (ref. code: 00-014-0613). However, the XRD patterns show the presence of a  $\text{MnVO}_3$  anorthic structure (ref. code 00-024-1260),  $\text{Zn}_3(\text{VO}_4)_2$  in an orthorhombic structure (space group Abam), with (ICDS ref. code: 00-034-0378),  $\text{BiVO}_4$  Orthorhombic with (ref. code 00-012-0293) space group P nca. These are in addition to the major phase of the ZnO hexagonal structure.

### 3.2 Microstructure Characterizations

Fig. 2 (a to c) shows the microstructure of the sample with 0.08, 0.2 and 0.4 mol% of  $\text{V}_2\text{O}_5$  content; all the ceramics were sintered at 1250 °C. The microstructure of the ceramics are well pronounced. Thus, the average grain size decreased gradually from 24.79 to 17.22  $\mu\text{m}$  with increased in  $\text{V}_2\text{O}_5$  content. This may likely be due to the presence of the  $\text{Zn}_7\text{Sb}_2\text{O}_{12}$  spinel phase that can inhibit the ZnO grain growth [34]. The presence of pores decreased the relative density from 5.32 to 5.06  $\text{g}/\text{cm}^3$ , for ceramic sintered at 1200 – 1300 °C may be this happen as a result of  $\text{V}_2\text{O}_5$  volatility [12, 23] during sintering. Also, for 0.08 - 0.4 mol%  $\text{V}_2\text{O}_5$  dopants sintered at 1250°C, maximum density of 5.12  $\text{g}/\text{cm}^3$  was observed from the ceramic doped with 0.2 mol%  $\text{V}_2\text{O}_5$ , see Table 1 below.

The EDX analysis confirmed the presence of Zn, Mn, V, Bi and Sb elements at the grain interior, grain boundaries and triple point junction coexisting in bulk Zn grains; Fig. 3, spectrum

(1, 2 and 3). Although it was reported that no V species was located in the ZnO grains' interior [18].

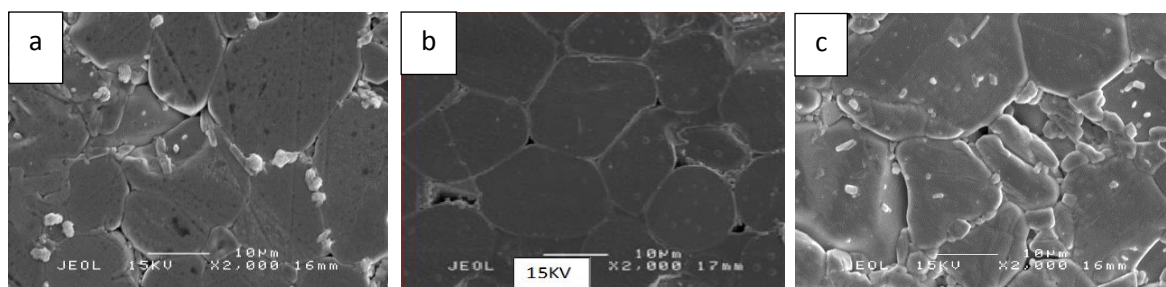


Fig. 2: Microstructure of  $V_2O_5$  doped ZBSM based ceramics (a) 0.08 mol%, (b) 0.2 mol% and (c) 0.4 mol% sintered at 1250 °C

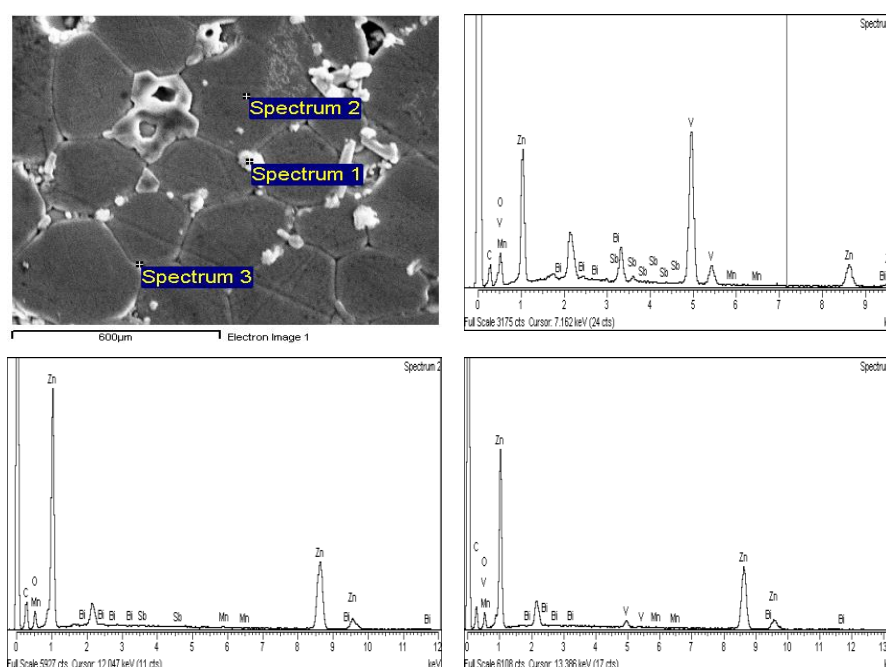


Fig. 3: EDX spectra for sample of 0.2 mol% of  $V_2O_5$  content sintered at 1200 °C

Evidently from Fig. 4, a clear grain, with the exception of grain size, was monitored. The grain size and shape of the ceramics sintered at 1200 °C were different. The sample shows two different types of grains, the bulk grain ZnO phase and the inter-granular phase with defects concentrated on the surface. This result is consistent with the previous work [30]. During the sintering, the material was in thermodynamic equilibrium; so, there was a high Schottky type. Therefore, the defects formed on the surfaces on the bulk grains during cooling and annihilation [31]. The vanished defect concentration was mainly composed of V-species which were located at the triple junctions, this was confirmed by the EDX analysis in Fig. 4 (spectrum 1). When the temperature increased from 1250 to 1300 °C, the inter-granular phase disappearance detected and this is due to the high reactivity of the V-species at a higher temperature, which can be found in the grain boundary EDX analysis (spectrum 2). However, the average grain size increased to a maximum of 31.39  $\mu\text{m}$  at 1300 °C. This was caused by the V-species that possibly melted easily on the ZnO grains interior leading to the exaggerated ZnO grains [32]. The exaggeration of the ZnO grain was potentially contributed to by the addition of  $V_2O_5$  and its lower melting point (690

°C). This was a clear fact on the sample sintered at temperatures higher than the temperature at which the liquid phase occurred [33]. The presence of pores was attributed to the volatility of  $V_2O_5$  at higher temperatures.

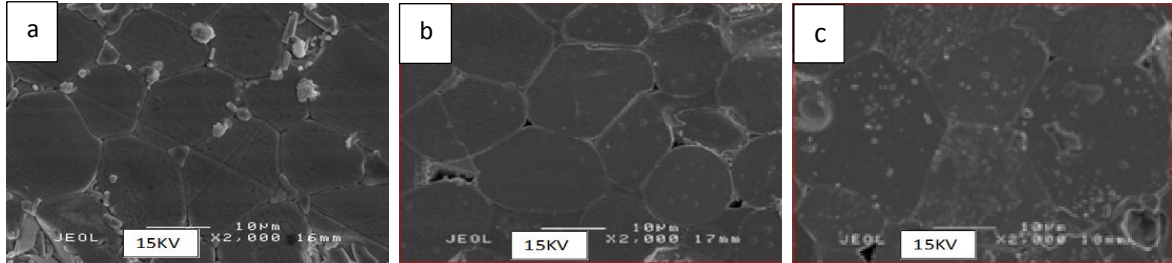


Fig. 4(a – c): SEM micrographs of the  $V_2O_5$  doped ZBSM ceramics sintered between 1200-1300 °C

### 3.3 Electrical Characterization

Fig. 5(a) showed the J-E characteristic curve of sample sintered between 1200-1250 °C and doped at 0.2 mol% and Fig. 5(b) that of doped at 0.08, 0.2, 0.4 mol% and sintered at optimum temperature, 1250 °C. The electrical properties, such as  $\alpha$ ,  $\phi_b$ ,  $J_L$ ,  $E_b$ , and microstructure properties, such as average grain size and relative density are summarized in Table 1.

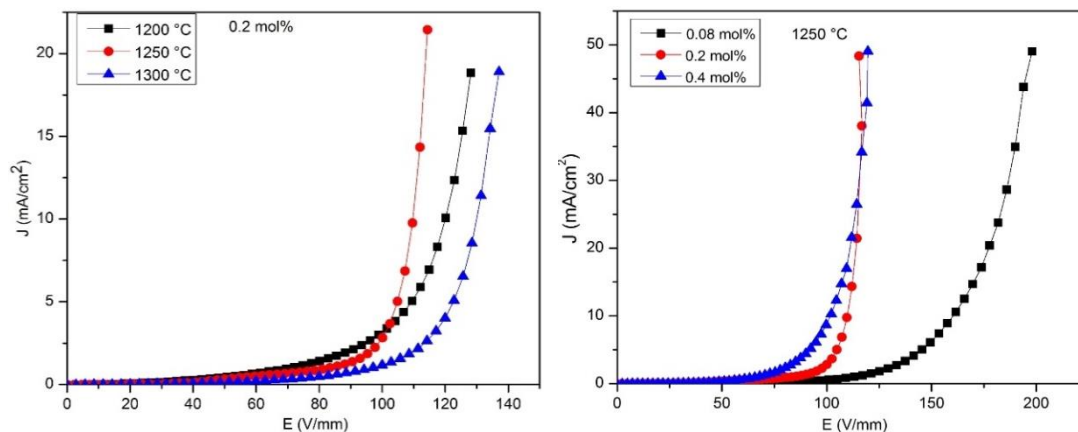


Fig. 5: The J-E characteristics curve of the ceramics samples (a) doped with 0.2 mol%  $V_2O_5$  sintered between temperature 1200-1300 °C and (b) doped between 0.08, 0.2 and 0.4 mol%  $V_2O_5$  at 1250 °C.

The  $\alpha$  results confirmed 1250 °C as the optimum sintering temperature with composition 0.2 mol% of  $V_2O_5$  doped ZBSM ceramics sintered between 1200-1300 °C. However, at an optimum sintering temperature 1250 °C varying the dopants from 0.08 and 0.4 mol% the  $\alpha$  does not significantly improved in comparison to 0.2 mol% of  $V_2O_5$  doping. This means that sintering temperature 1250 °C and 0.2 mol% of  $V_2O_5$  doped ZBSM is the optimum condition to achieve  $\alpha$  value in the current process condition. The  $\alpha$  value of 12.18 was accompanied by lowest  $J_L$  around  $1 \times 10^{-4}$  mA/cm<sup>2</sup> and a maximum  $\phi_b$  of 1.38 eV; the larger the  $\phi_b$  is the better is the  $\alpha$  value [35]. Fig. 5(a) and (b) show the relation between  $\phi_b$ ,  $E_b$  and  $\alpha$  as a function of temperature. Further increasing the sintering temperature caused  $\alpha$  to decrease to 3.30 at 1300 °C. This was associated with the partial disappearance of the grain boundaries caused by a large growth of ZnO grains at a high temperature, which caused the reduction of  $E_b$  to 12.10 V/mm and the  $J_L$  to increase to a maximum value of  $6 \times 10^{-4}$  mA/cm<sup>2</sup>. The increase in grain size led to the retardation of the grain boundaries which can hinder it and cause a poor performance of the ZnO varistor ceramics [13 – 20]. Table (1) shows the electrical parameters for the samples with and without  $V_2O_5$  contents. In

addition, the homogeneity of the sintered sample contributed to the variation of the electrical properties of the individual grain boundary, particularly at 1250 °C

*Table 1: Electrical and microstructural properties for the V<sub>2</sub>O<sub>5</sub> doped of ZBSM based varistor ceramics sintered at various temperatures and compositions.*

V <sub>2</sub> O <sub>5</sub> doping (mol%)	Sintering temperature (°C)	d (μm)	ρ (g/cm <sup>3</sup> )	φ <sub>b</sub> (eV)	E <sub>b</sub> (V/mm)	J <sub>L</sub> (mA/cm <sup>2</sup> )	α
0.2	1200	12.02	5.32	0.53	22.90	3×10 <sup>-4</sup>	5.51
	1225	14.87	5.28	0.65	60.50	2×10 <sup>-4</sup>	10.37
	1250	20.99	5.22	1.38	50.20	1×10 <sup>-4</sup>	12.18
	1275	22.81	5.11	0.47	39.20	2×10 <sup>-4</sup>	8.63
	1300	31.39	5.06	0.46	12.10	6×10 <sup>-4</sup>	3.31
0.08	1250	23.09	5.02	1.00	56.95	1×10 <sup>-4</sup>	7.78
0.4	1250	17.22	5.12	1.03	32.0	1×10 <sup>-4</sup>	8.67

In addition, the homogeneity of the sintered ceramics contributed to the variation of the nonlinear electrical properties of the individual grain boundary, particularly at 1250 °C with 0.2 mol% V<sub>2</sub>O<sub>5</sub> doped ZBMS [36]. It is a clear indicator that that the nonlinear electrical properties of the ZnO varistor are influenced by its microstructure as shown in the SEM micrographs, Figs. 3 and 4.

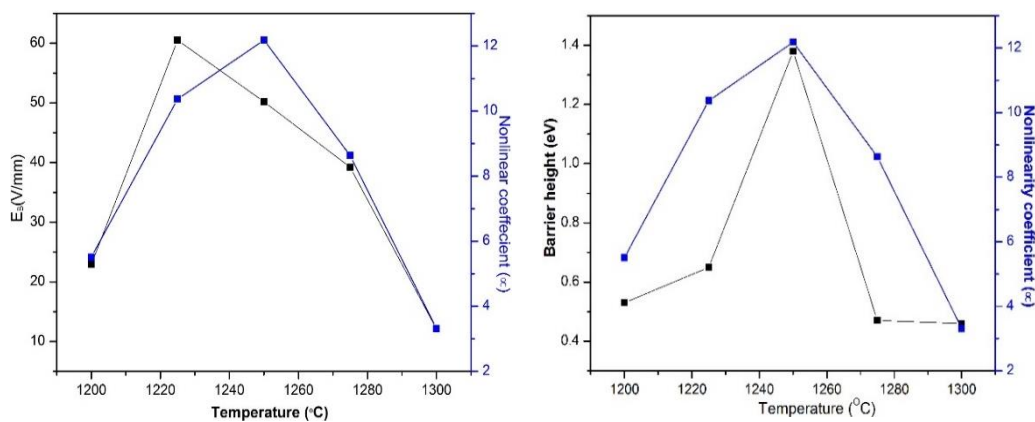


*Fig. 6: The relationship between (a) E<sub>b</sub>, α, and (b) φ<sub>b</sub>, α, with sintered temperatures (1200-1300 °C).*

## Conclusion

The effect of the sintering temperature ranging from 1200 to 1300 °C and the composition of V<sub>2</sub>O<sub>5</sub> (0.08 to 0.4 mol%) on the ZBSM based varistor ceramics was investigated. The results indicated that the optimum temperature that give the best in term of microstructure and electrical properties is at 1250 °C with 0.2 mol% of V<sub>2</sub>O<sub>5</sub>. Then by varying the dopant composition at this temperature it was observed that 0.2 mol% also give the optimum microstructure and electrical properties. The ceramic sintered at 1250 °C and 0.2 mol% of V<sub>2</sub>O<sub>5</sub> exhibited the largest φ<sub>b</sub>, low J<sub>L</sub> with the best α around 12.18 and the E<sub>b</sub> of 50.20 V/mm.

## Acknowledgement

The authors are grateful to the Universiti Putra Malaysia for supporting this work under the Universiti Putra Malaysia grant No. GP-IBT/2013/9421100.

## References

- [1] A. Sedky, M. Abu-Abdeen, A. A. Almulhem *Phys. B Condens. Matter* **388**(1-2), 266 (2007).
- [2] V. O. Varistor, C. Diao, S. Chien, C. Yang, H. Chan, Y. Chen, and H. Chung *Key Engineering Materials* **372**, 493 (2008).
- [3] J. O. Akinnifesi and O. O. Akinwunmi *J. Mater. Sci. Res.* **3**(40), 40 (2015).
- [4] M. Dorraj, A. Zakaria, Y. Abdollahi, M. Hashim, and S. Moosavi *Sci. World J.* **20**(14), 9 (2014).
- [5] C. Leach, Z. Ling, and R. Freer *J. Eur. Ceram. Soc.* **16**, 2759 (2000).
- [6] H. H. Hng and P. L. Chan *Mater. Chem. Phys.* **75**(1-3), 61 (2002).
- [7] O. A. Desouky, S. E. Mansour, E. M. Negim, A. M. Najjar, R. Rakhmetullayeva, P. I. Urkimbaeva, and W. Midlands *World J. Chem.* **8**(2), 33 (2013).
- [8] T. Asokan, G. N. K. Iyengar, and G. R. Nagabhushana, *J. Mater. Sci.* **22**(6), 2229 (1987).
- [9] C. H. Lu, N. Chyi, H. W. Wong, and W. J. Hwang, *Mater. Chem. Phys.* **62**(2), 164 (2000).
- [10] H. Pfeiffer and K. M. Knowles *J. Eur. Ceram. Soc.* **24**(6), 1199 (2004).
- [11] Y. W. Hong and J. H. Kim, *Ceram. Int.* **30**(7), 1301 (2004).
- [12] J. H. Ju, H. Wang, and J. W. Xu *Adv. Mater.* **320**, 240 (2011).
- [13] H. H. Hng and K. Y. Tse *J. Mater. Sci.* **38**(11), 2367 (2003).
- [14] G. Chen, X. Chen, X. Kang, and C. Yuan *J. Mater. Sci. Mater. Electron.* **26**(4), 2389 (2015).
- [15] C. W. Nahm *Ceram. Int.* **39**(2), 2117 (2013).
- [16] C. W. Nahm *J. Mater. Sci. Mater. Electron.* **23**(2), 457 (2012).
- [17] C. W. Nahm *J. Mater. Sci. Mater. Electron.* **19**(10), 1023 (2008).
- [18] C. Kuo, C. Chen, and I. Lin *J. Am. Ceram. Soc.* **81**(11), 2942 (1998).
- [19] H. H. Hng and P. L. Chan *Ceram. Int.* **30**(7) 1647 (2004).
- [20] J.-K. Tsai and T.-B. Wu *J. Appl. Phys.* **76**(8) 4817 (1994).
- [21] R. A. Winston and J. F. Cordaro *J. Appl. Phys.* **68**(12), 6495 (1990).
- [22] M. Mirzayi and M. H. Hekmatshoar *Phys. B Condens. Matter* **414**, 50 (2013).
- [23] M. Peiteado, J. F. Fernández, and A. C. Caballero *J. Eur. Ceram. Soc.* **27**(13-15), 386 (2007).
- [24] H. H. Hng and K. M. Knowles *J. Am. Ceram. Soc.* **83**(10), 2455 (2000).
- [25] C.-S. Chen, C.-T. Kuo, and I.-N. Lin *J. Mater. Res.* **13**(06), 1560 (2011).
- [26] A. Gubański, W. Mielcarek, K. Prociów, J. Warycha, J. M. Wróbel *Material Science-Poland* **27**(4/2), 1207 (2009)
- [27] M. G. M. Sabri, B. Z. Azmi, Z. Rizwan, M. K. Halimah, M. Hashim, M. H. M. Zaid *Int. J. Phys. Sci.* **6**(6), 1388 (2011).
- [28] A. Badev, S. Marinell, R. Heuguet, E. Savary, and D. Agrawal *Acta Mater.* **61**(20), 7849 (2013).
- [29] Y. W. Lao, S. T. Kuo, and W. H. Tuan, *J. Electroceramics* **19**(2-3), 187 (2007).
- [30] P. Q. Mantas and J. L. Baptista *J. Eur. Ceram. Soc.* **15**(7), 605 (1995).
- [31] F. Kharchouche, D. E. C. Belkhiat, and S. Belkhiat *IET Sci. Meas. Technol.* **7**(6), 326 (2013).
- [32] H. H. Hng and L. Halim *Materials letter.* **57**(8), 1411 (2003).
- [33] S. Bernik, N. Daneu, and a. Rečnik *J. Eur. Ceram. Soc.* **24**(15-16), 3703 (2004).
- [34] R. Guo, L. Fang, H. Zhou, X. Chen, D. Chu, B. Chan, and Y. Qin *J. Mater. Sci. Mater. Electron.* **24**(8), 2721 (2013).
- [35] F. Jiang, Z. Peng, Y. Zang, and X. Fu *J. Adv. Ceram.* **2**(3) 201 (2013).
- [36] C. Zhang, Y. Hu, W. Lu, M. Cao, and D. Zhou *J. Eur. Ceram. Soc.* **22**(1), 61 (2002).